

# Influence of high energy electron irradiation on the characteristics of polysilicon thin film transistors

P.V. Aleksandrova<sup>a</sup>, V.K. Gueorguiev, Tz.E. Ivanov, and S. Kaschieva

Institute of Solid State Physics, Bulgarian Academy of Sciences, 72 Tzarigradsko Chaussee Blvd., 1784 Sofia, Bulgaria

Received 14 April 2006 / Received in final form 10 July 2006

Published online 2 August 2006 – © EDP Sciences, Società Italiana di Fisica, Springer-Verlag 2006

**Abstract.** The influence of high energy electron (23 MeV) irradiation on the electrical characteristics of *p*-channel polysilicon thin film transistors (PSTFTs) was studied. The channel 220 nm thick LPCVD (low pressure chemical vapor deposition) deposited polysilicon layer was phosphorus doped by ion implantation. A 45 nm thick, thermally grown, SiO<sub>2</sub> layer served as gate dielectric. A self-alignment technology for boron doping of the source and drain regions was used. 200 nm thick polysilicon film was deposited as a gate electrode. The obtained *p*-channel PSTFTs were irradiated with different high energy electron doses. Leakage currents through the gate oxide and transfer characteristics of the transistors were measured. A software model describing the field enhancement and the non-uniform current distribution at textured polysilicon/oxide interface was developed. In order to assess the irradiation-stimulated changes of gate oxide parameters the gate oxide tunneling conduction and transistor characteristics were studied. At MeV dose of  $6 \times 10^{13}$  el/cm<sup>2</sup>, a negligible degradation of the transistor properties was found. A significant deterioration of the electrical properties of PSTFTs at MeV irradiation dose of  $3 \times 10^{14}$  el/cm<sup>2</sup> was observed.

**PACS.** 61.80.Fe Electron and positron radiation effects – 72.20.-i Conductivity phenomena in semiconductors and insulators – 73.20.At Surface states, band structure, electron density of states

## 1 Introduction

Polycrystalline silicon thin film transistors (PSTFTs) are of considerable importance because of their use in active-matrix crystal displays, charge coupled devices (CCDs) and large-area electronic devices. Recently, it has been reported that the PSTFT technologies are promising for fabrication of high performance submicron transistors [1].

The effects of radiation damages on various electronic devices have been investigated in order to examine their radiation resistance [1–7]. The necessity of stable under irradiation electronic devices for applications in space apparatuses, avionics, nuclear power plants instrumentation, high energy physics instruments and etc. increases. Radiation-induced defects alter the structural properties of materials and the electrical properties of devices [2]. Several researchers have verified the degradation of TFTs after gamma-ray irradiation [3,4]. It has been reported that the gate oxide quality after electron-beam irradiation is significantly degraded [5]. The thin gate oxides of submicron technologies are inherently more tolerant to the radiation-stimulated defects than the thicker oxides used in less advanced technologies [6,7].

It is well-known that gate oxides grown on polycrystalline silicon (polyoxides) conduct much higher currents

than oxides grown on monocrystalline silicon. The increased oxide conductivity is due to the rough texture of polysilicon surface and asperities at polysilicon/polyoxide interfaces. The interface asperities increase the local electric field. A quantitative and qualitative model, describing the higher and non-uniform conductivity through thermal oxides grown on polycrystalline silicon, has been proposed from Groeseneken and Maes [8]. The model is based on a combination of the conventional Fowler-Nordheim conduction mechanism and a first-order kinetic trapping model. It is able to explain the trapping phenomena and the non-uniform distribution of leakage currents through the polyoxides.

In the recent study, the electrical properties of high-energy electron irradiated PSTFTs were studied. In order to calculate the radiation-stimulated degradation of the electrical properties of PSTFTs a computer program, based on the model of Groeseneken and Maes, was developed.

## 2 Experiment

The studied PSTFTs were fabricated on 220 nm thick polysilicon layer deposited on thermally oxidized silicon wafers by LPCVD using SiH<sub>4</sub> source gas at 620 °C and pressure about 0.4 Torr. The wafers were oxidized and

<sup>a</sup> e-mail: val@issp.bas.bg

annealed at 1000 °C for 3 h in dry N<sub>2</sub> ambient for grain enlargement. Transmission electron microscopy analysis showed that the polysilicon layers have a columnar structure with average grain size of about 100 nm. Through the thin SiO<sub>2</sub> layer, the polysilicon was phosphorus implanted at energy of 85 keV and dose  $1 \times 10^{12}$  cm<sup>-2</sup>. The oxide layer was then removed and SiO<sub>2</sub> with thickness 45 nm was grown at 1000 °C in dry oxygen as a gate dielectric. The final thickness of the channel polysilicon layer was about 150 nm. The source and drain regions were heavily doped by self-aligned boron ion implantation with dose  $>10^{15}$  cm<sup>-2</sup>. As a gate electrode 200 nm thick *n*+polysilicon was deposited. Then 100 nm thick oxide layers were deposited by LPCVD as a cap layer. After opening the contact holes, Al/Si was deposited, sintered and patterned. *p*-channel PSTFTs with channel width  $W = 50$  μm and length  $L = 50$  μm were fabricated and investigated.

Three groups of *p*-channel PSTFTs were irradiated with 23 MeV electrons at a flux of about  $10^{12}$  el/cm<sup>2</sup> s. The first group of samples /dose.1/ was irradiated with 23 MeV electrons for 60 s. The second group was irradiated with 23 MeV electrons for 300 s /dose.2/. The beam current in the both cases was  $I_e = 6$  μA. The third group of the samples /dose.3/ was irradiated with 23 MeV electrons for 600 s and the beam current was  $I_e = 3$  μA. In this way the samples from the second and third group were irradiated with equal dose electrons, but for different time duration.

Electron irradiation was carried out with the Microtron MT-25 at the Flerov Laboratory of Nuclear Reactions of Joint Institute of Nuclear Research, Dubna, Russia. The electron irradiation was completed in vacuum ( $10^{-3}$  atm). The distance between the Microtron window and the sample was 150 nm. Current-voltage (*I*-*V*) characteristics of the transistors were measured by a programmable Keithley 617 electrometer.

### 3 Model

A computer program, based on the model of Groeseneken and Maes describing the conductivity of polyoxides, was developed. More details about the model can be found in [8]. The model describes the natural field enhancement at the silicon/silicon dioxide interface, which is observed in oxides, thermally grown on top of polycrystalline silicon layers. The increase of the local electric field at any position in the oxide is due to the textured polyoxide/polysilicon interface.

The program solves selfconsistently the following equations described in the model of Groeseneken and Maes:

$$\frac{\partial n_t(x, t)}{\partial t} = \frac{\sigma}{q} J(x, t) [N_t - n_t(x, t)] \quad (1)$$

$$\frac{\partial n_t(x, t)}{\partial t} = \frac{\partial J(x, t)}{\partial x} \quad (2)$$

where  $N_t$  is the density of oxide traps,  $\sigma$  is the capture cross-section of traps,  $n_t(x, t)$  is the filled trap density,

$J(x, t)$  is the position-dependent current density and  $q$  is the electronic charge. It is assumed that the density of traps  $N_t$  is uniform over the oxide thickness and independent of time. The increase of the number of filled trap centers  $n_t(x, t)$  with the time, due to the injected current carriers, is described by equation (1). The decrease of the current density  $J(x, t)$  due to the captured carriers, is given in equation (2).

The current conduction mechanism at local electric field  $E_{inj}$  at the injecting polyoxide/polysilicon interface is expressed by the well-known Fowler-Nordheim tunneling equation:

$$J = C E_{inj}^2 \exp\left(-\frac{E_c}{E_{inj}}\right) \quad (3)$$

where  $C$  and  $E_c$  are constants determined by the oxide properties [8].

The local electric field  $E_{inj}$  is calculated by the applied voltage  $V_a$ , trapping voltage  $V_q$ , oxide thickness  $t_{ox}$  and the local field enhancement factor  $\mu$ :

$$E_{inj} = \mu \frac{(V_a - V_q)}{t_{ox}} \quad (4)$$

The trapping voltage  $V_q$  is used as a correction parameter in the calculation of the local electric field due to the captured carriers. The applied voltage  $V_a$  is calculated by the flat-band voltage  $V_{FB}$  and the substrate potential  $\phi_F$  as:

$$V_a = V_g - V_{FB} - 2\phi_F \quad (5)$$

for inversion mode and

$$V_a = V_g - V_{FB} - 0.55 + \phi_F \quad (6)$$

for accumulation mode of the transistors.

The trapping voltage, calculated from the density of filled traps,  $V_q$  is expressed by:

$$V_q = \frac{Q_T \bar{x}}{\varepsilon_{ox}} \quad (7)$$

where  $Q_T$  is the trapped charge given by

$$Q_T = q \int_0^{tox} n_t(x) dx \quad (8)$$

and  $\bar{x}$  is the charge centroid, which is calculated from the distribution of filled trap centers.

It is assumed that the rough polysilicon/polyoxide interface consists of rather small asperities with identical shapes. Each asperity is divided into *i*-regions with a constant field enhancement factor  $\mu_i$ . The field enhancement factor  $\mu_i$  depends on the position of the *i*-region over the asperity. The trapped charge  $Q_{Ti}$ , trapping voltage  $V_{qi}$ , injection field  $E_{inj i}$  and field enhancement factor  $\mu_i$  is calculated for each *i*-region. The field enhancement factor  $\mu_i$  appears over the same fraction of the total interface area, due to the assumption of identical asperity shape.

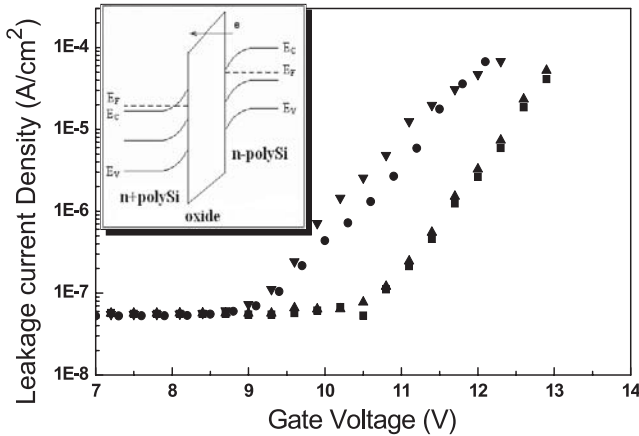


Fig. 1. Leakage currents at positive voltage scanning: ● — nonirradiated, ▼ — dose.1, ▲ — dose.2, ■ — dose.3 samples.

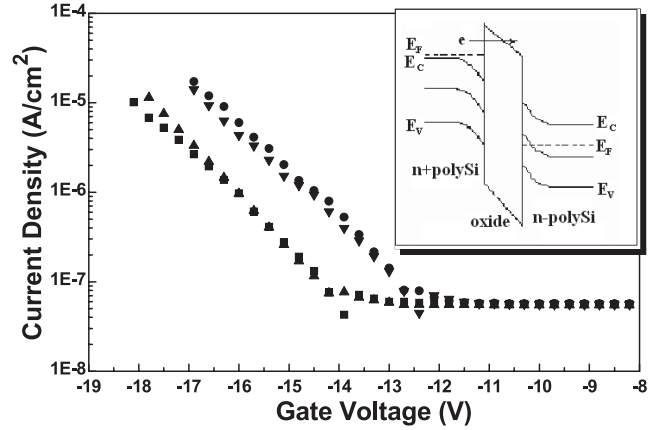


Fig. 2. Leakage currents at negative voltage scanning: ● — nonirradiated, ▼ — dose.1, ▲ — dose.2, ■ — dose.3 samples.

The used input parameters are  $N_t$ ,  $\sigma$ ,  $t_{ox}$ ,  $\mu$ ,  $V_a$ ,  $C$  and  $E_c$ . In this way, a nonuniform current, a nonuniform field distribution and a nonuniform trapped charge density over the interface area are obtained.

An area distribution function  $P(\mu_i)$  is used in order to calculate the total current density. Groeseneken and Maes have found that the best fits with the experimental data can be obtained with an exponential decreasing form of the area distribution function  $P(\mu_i)$ , given by

$$P(\mu_i) = K \cdot \exp(-(\mu_i - 1)/\mu_0) \quad (9)$$

where  $\mu_0$  is a mean value of the parameter  $\mu_i$  and  $K$  is a constant.

The numerical solution of the second trapping differential equation (2) yields the position-dependent current density. The position-dependent current density is then used in the solution of the first trapping differential equation (1). After calculation of all partial current densities ( $J_p$ ) at any position at the interface, the total current density is obtained as a sum of all  $J_p$  each multiplied by its respective area distribution function  $P(\mu_i)$ .

The model of Groeseneken and Maes allows being derived two main parameters of the polyoxides and polysilicon/polyoxide interfaces — the mean field enhancement factor  $\mu_0$  and the trapping probability  $P_t = t_{ox}N_t\sigma$ . The parameters  $P_t$  and  $\mu_0$  are a relative estimation of the oxide quality and interface roughness, respectively. Thus, the influences of different technology treatments on the gate oxide quality and interface roughness can be compared.

#### 4 Experimental results and discussion

The energy band bending of the experimental  $n+$ -polySi/SiO<sub>2</sub>/ $n$ -polySi structure at positive and negative gate voltages is shown in the insert of Figures 1 and 2, respectively. When, to the  $n+$ -polySi gate a positive voltage is applied, the initial band bending caused by the built-in positive oxide charge increases. The accumulated electrons at the  $n$ -polySi surface are injected

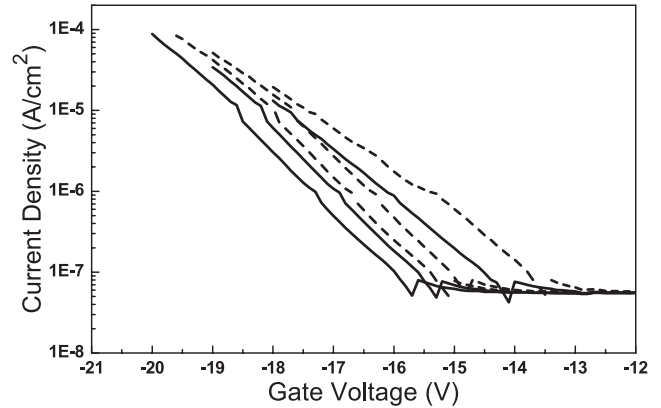


Fig. 3. Comparison between nonirradiated (dash line) and dose.2. (straight line) samples.

into the oxide. In this case, the quality of the bottom  $n$ -polySi/SiO<sub>2</sub> interface can be estimated. When, on the  $n+$ -polySi gate is applied a negative voltage, the bands at  $n$ -polySi/SiO<sub>2</sub> interface will be bent up. The electrons will be injected into the oxide from the gate electrode. In this case, the electron injection gives information about the properties of the  $n+$ -polySi/SiO<sub>2</sub> interface.

The measured leakage curves on nonirradiated and irradiated samples, at the first positive and negative ramp, are shown in Figures 1 and 2, respectively. The first current-voltage ( $I$ - $V$ ) ramp of samples dose.2 and dose.3 coincides. The total irradiation dose of dose.2 and dose.3 samples is equal, only the irradiation time is different. Therefore, the quantity of irradiation-stimulated defects is proportional to the total dose of irradiation and does not depend on the time of irradiation.

Typical  $I$ - $V$  characteristics, measured on nonirradiated and irradiated samples at three consecutive voltage ramps, are shown in Figure 3. At the first ramp, the electron tunneling starts at lower applied voltages in comparison with the second and third ramp. During the first ramp, the trapped carriers in the oxide partially compensate the injection field increasing the trapping voltage. At the following ramp, the electron tunneling occurs at higher

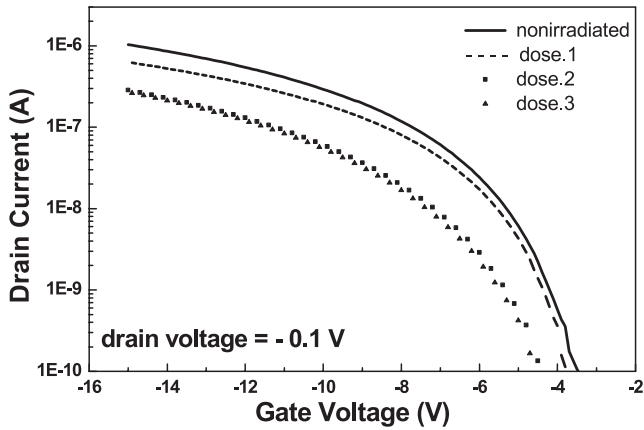


Fig. 4. Transfer characteristics of PSTFTs.

Table 1.

Sample	$R$ , $k\Omega/\square$	$V_{th}$ , V	$Q_{tot}$ , $10^{12} \text{ cm}^{-2}$	$\Phi_B$ , eV
C15 non	$10 \times 10^3$	-2,7	1.44	0.38
C15 dose1	$12.5 \times 10^3$	-2,8	1.5	0.38
C15 dose2	$25 \times 10^3$	-3,6	1.89	0.36
C15 dose3	$33 \times 10^3$	-3,8	2	0.35

electric field. Moreover, at the first ramp, the leakage current rises less steeply than the typical Fowler-Nordheim curve due to the trapped electrons and injection field shielding.

The measured  $I$ - $V$  characteristics on the irradiated samples show that the electron injection starts at higher voltages (Figs. 1–3). In the low-level leakage current region, the electrons are trapped into the irradiation-generated defects. During the voltage ramp, the captured electrons in the irradiation-stimulated defects lead to increase of the trapping voltage  $V_q$  and, consequently, to a decrease of the injection field  $E_{inj}$ . Therefore, the leakage curve shift is due to the oxide charge increase. The irradiation-stimulated defects in the gate oxide could be interpreted as positively charged trapping centers.

The influence of MeV irradiation on the transfer characteristics of PSTFTs is shown in Figure 4. The threshold voltages  $V_{th}$  were calculated from the transfer characteristics. The obtained flat-band voltage values were used in equations (5) and (6). The values of total oxide charge  $Q_{tot}$  at different irradiation doses were calculated using well-known equations from the MOS transistors theory, giving a relationship between flat-band voltage and oxide charge. The results are shown in Table 1. The values of the interface charge and oxide charge could not be separated by the used equations, then, the calculated  $Q_{tot}$  consists of the both parameters.

It was shown [9] that 11 MeV electron irradiation creates a new spectrum of interface states in the monocrystalline silicon band gap at the Si/SiO<sub>2</sub> interface. Probably, the same effect could be expected at the polyoxide/polysilicon interface, but further experiments are needed.

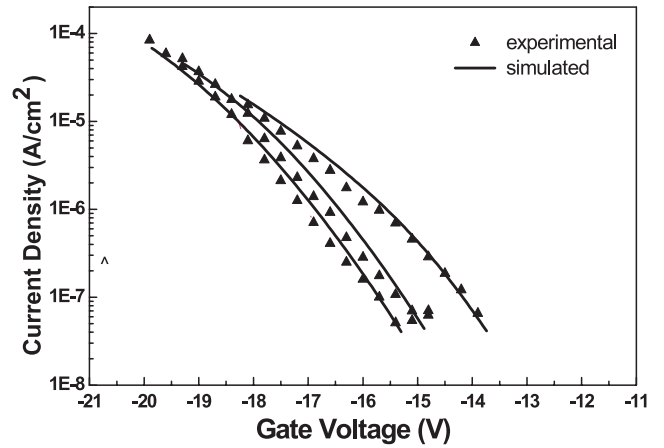


Fig. 5. Leakage currents at three consecutive negative voltage ramps on nonirradiated sample.

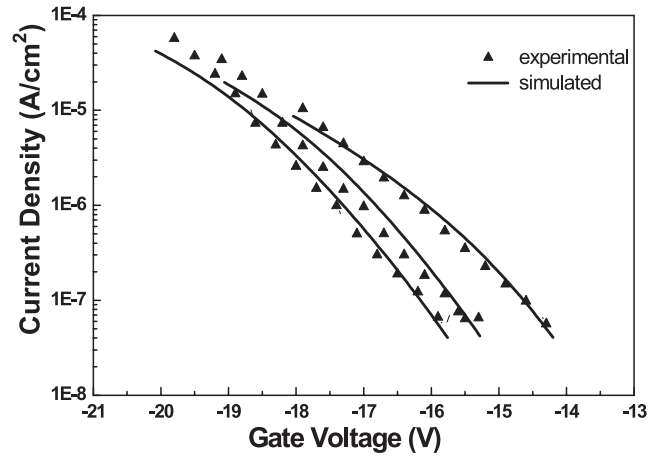


Fig. 6. Leakage currents at three consecutive negative voltage ramps on irradiated with dose.2 sample.

The negative threshold voltage shift, corresponding to the different irradiation doses, confirms the increase of the total positive oxide charge. The radiation-stimulated damages decrease also the bulk potential ( $\Phi_B$ ). This effect can be explained by type conversion effects in the polysilicon channel layer [2]. The channel resistance increase is due to the induced displacement-damages during the irradiation. High-energy electron radiation can displace Si atoms from their lattice positions, creating displacement damages. This process affects the properties of the bulk polysilicon. These bulk damages are responsible to the increase of defect states in the thin layers.

Typical simulated  $I$ - $V$  characteristics of nonirradiated and dose.2 samples are shown in Figures 5 and 6, respectively. The applied voltage ramps are negative. Satisfactory agreement between measured and simulated curves can be seen. Similar experimental coincidences of the measured leakage curves, at three consecutive voltage ramps, on nonirradiated and irradiated samples were observed.

By simulation of the experimental  $I$ - $V$  curves, some physical parameters of polyoxides were obtained. The data are summarized in Table 2. Three essential parameters are

Table 2.

	Sample	$\mu_0$	$P_t, 10^{-2}$	$N_t, 10^{18} \text{ cm}^{-3}$
Positive ramps	C15 non	0.45	3	1.3
	C15 dose1	0.5	6.75	3
	C15 dose2	0.4	33.75	15
	C15 dose3	0.4	45	20
Negative ramps	C15 non	0.23	0.7	0.3
	C15 dose1	0.23	0.7	0.3
	C15 dose2	0.24	1.6	0.7
	C15 dose3	0.26	3	1.2

further discussed — mean field enhancement factor  $\mu_0$ , trapping probability  $P_t$  and density of oxide traps  $N_t$ .

The mean field enhancement factor  $\mu_0$  at the bottom interface is higher, it is related to the rougher bottom interface. The factor  $\mu_0$  at the bottom interface slightly decreases with increasing of the irradiation doses. Therefore, the initially rough interface becomes smoother during the irradiation. Possibly, it is due to slight oxidation of the polysilicon surface. Similar effect has been already reported for thermally oxides grown on monocrystalline silicon [10]. Kurmaev et al. [10] have proposed that during MeV irradiation oxygen atoms can replace silicon ones, because of break of Si–Si bonds.

In order to determine the oxide thickness, capacitance-voltage measurements were performed. The results showed that there is no an essential change of the oxide thickness. Thus, the increase of the thickness of SiO<sub>2</sub> grown on poly-Si is lower than the increase of the thickness of SiO<sub>2</sub> on monocrystalline silicon.

The factor  $\mu_0$  at the top interface increases with the irradiation dose. During the irradiation, the initially smoother interface becomes rougher.

The trapping probability  $P_t$  estimates the quality of gate oxides. The higher  $P_t$  value corresponds to lower quality of the gate oxide. At the both interfaces, the calculated  $P_t$  values are different. At the top interface,  $P_t$  is lower than that at the bottom interface. The parameter  $P_t$  of the nonirradiated samples is about 3 times higher than that at the top interface. The obtained result can be related with the well-known deficiency of oxygen at the bottom interface.

The used model does not calculate the values of density of states and capture cross-section of traps separately only their product — the trapping probability. It is reasonable to assume that the irradiation changes the capture cross-section of traps  $\sigma$ . The used  $\sigma$  value —  $1 \times 10^{-18} \text{ cm}^2$ , typical for the nonirradiated oxides, shows a good coincidence with the experimental data. Thus, the density of traps is a dominant factor in determining of the trapping probabilities.

At the bottom interface of the nonirradiated sample, the calculated  $N_t$  value is higher. At dose.3, the parameter  $N_t$  increases of about 15 times. While at the top interface,  $N_t$  value is lower. The charge centroid is located closer to the bottom interface. Therefore, the break of Si–Si bonds and the possible ionization of silicon, and oxygen atoms are predominantly located near the bottom interface.

## 5 Conclusions

The electrical characteristics of high-energy electron irradiated PSTFTs were studied. A computer program based on the model of Groeseneken and Maes was used to calculate the radiation-stimulated degradation of the gate oxide. Satisfactory agreement between the measured and simulated curves was demonstrated.

Four essential parameters estimating the influence of high-energy electron irradiation on the gate oxide were discussed—oxide charge, trapping probability, interface roughness and density of traps. The extracted parameters show an increase of the density of traps and the trapping probabilities with increasing of the irradiation dose. The irradiation-stimulated defects in the gate oxide (SiO<sub>2</sub>) act as positively charged trapping centers. The experimental data reveal an increase of about 17 times of the trap density and of about 30% of the positive oxide charge. The threshold voltage negative shift, after MeV irradiation, confirms the increase of positive oxide charge.

For MeV dose of  $6 \times 10^{13} \text{ el/cm}^2$ , no essential degradation of the transistor properties was found, while at MeV irradiation dose of  $3 \times 10^{14} \text{ el/cm}^2$  a significant deterioration of the electrical properties of PSTFTs was observed.

The financial support by the Bulgarian National Scientific Found under Contract MUF-1505 is gratefully acknowledged. The authors would like to thank JINR, Dubna, Russia for the fruitful collaboration.

## References

1. A.W. Wang, K.C. Saraswat, IEEE Trans. of El. Device **47**, 1035 (2000)
2. J.R. Srouf, C.J. Marshall, P.W. Marshall, IEEE Trans. on Nuclear Sci. **50**, 653 (2003)
3. N.A. Hastas, C.A. Dimitriadis, J. Brini, G. Kamarinos, V.K. Gueorguiev, S. Kaschieva, Microel. Reliab. **43**, 57 (2003)
4. S. Kaschieva, S.N. Dimitriev, Vacuum **69**, 87 (2003)
5. Hiu Yung Wong, *Radiation effects in hafnium oxide as MOS gate dielectric caused by e-beam lithography* (Dissertation, University of California, Berkeley)
6. N.S. Saks, M.G. Ancona, J.A. Modolo, IEEE Trans. Nucl. Sci. **33**, 1185 (1986)
7. N.S. Saks, M.G. Ancona, J.A. Modolo, IEEE Trans. Nucl. Sci. **31**, 1249 (1984)
8. G. Groeseneken, H.E. Maes, IEEE Trans. El. Devices **E-33**, 7 (1986)
9. S. Kaschieva, Nucl. Instr. Meth. Phys. Res. B **93**, 274 (1994)
10. E.Z. Kurmarev, S.N. Shamin, V.R. Galakhov, A.A. Makhnev, M.M. Kirilova, T.E. Kurrennykh, V.B. Vykhodets, S. Kaschieva, J. Phys.: Condes. Matter **9**, 6969 (1997)